
INVESTIGATING THE GEOTHERMAL POTENTIAL WITHIN BENUE STATE, CENTRAL NIGERIA, FROM RADIOMETRIC AND HIGH RESOLUTION AERO MAGNETIC DATA

Akinnubi, Tunde Daniel and Adetona A. Abbass

Department of Physics, Federal University of Technology Minna, Niger State

Corresponding author email: tundexx2006@gmail.com, tonabass@gmail.com

ABSTRACT

The study focuses on the analysis of high resolution Aeromagnetic data for the estimation of geothermal potential within the eastern part of Lower Benue Basin and correlating the results from the analysis of radiometric concentration data of the study area. The study area covers a total area of 18,150 km², six aeromagnetic sheets cover the area, major towns are Markudi, Gboko, Otukpo, Agena, Akwana and Katsina-Ala, it is bounded by latitude 7.00° and 8.00° and longitude 8.00° and 9.50°. The aeromagnetic data was subjected to Fourier analysis and then spectral analysis of 12 sub sections was carried out. From the spectral analysis, the depth to the top of magnetic sources varies from 0.28 Km to 0.36 Km while the depth to the bottom of magnetic sources varies from 5.52 Km to 9.63 Km. The modified Curie depth method was employed in evaluating the Curie point depth, heat flow and geothermal gradient were also obtained. The region found to have a shallow Curie depth of 9 km at the south-western and south-eastern part of the study area has an average geothermal heat flow 103.98 Wm⁻². The geothermal gradient also has a value of 62°C/km and 30°C/km respectively with an average value of 41.59 °C/km, anomalous high heat flow of 153.35, and 135.62 Wm⁻² was obtained within around Katsina- Ala and Oturkpo respectively. Correlating this result with the analysis of the radiometric values covering the study area, the ternary map shows that potassium and thorium radioactive content is noticeably high within these areas where relatively high heat flow values were obtained, The radioactive heat production within the two geothermally active areas was estimated to be 1.47 μW/m³ and 2.21 μW/m³ respectively this can be associated with the occurrence of these elements.

Keywords: Geothermal potential. Heat flow, Ternary map.

1. INTRODUCTION

The reliability of geothermal energy source and its efficiency in the generation of electricity cannot be overemphasised, generally the knowledge of the geothermal gradient of an area helps in determining the suitability of such location for sitting geothermal plants for the generation of electricity that can be utilised for industrial, domestic and recreational activities (Adedapo

et al., 2013).

Among all other sources, the earth's heat is believed to have being derived from the decay of radioactive isotopes of uranium, thorium, potassium elements, as well as heat released from the electromagnetic effects of the earth's magnetic field and heat released during tidal force on the earth as it spins along its axis and rotates since the land cannot flow like water, it compresses

and distorts thereby generates heat (Adedapo et al., 2013).

The study of subsurface temperature, geothermal gradients and heat flow in association to the Curie-Point Depth (CPD) is crucial in understanding the thermal maturation of sediments and the past thermal regimes in a basin. Measurements have shown that a region with significant geothermal energy is characterised by an anomalous high temperature gradient and heat flow (Tselentis et al., 1991).

The Depth to Bottom Magnetic Source (DBMS) or Curie Point Depth (CPD) is known as the depth at which the dominant magnetic mineral in the crust passes from a ferromagnetic state to a paramagnetic state under the effect of increasing temperature (where the magnetisation is lost) (Nagata, 1961; Ofor and Udensi, 2014). It is therefore expected that geothermically active areas would be associated with shallow Curie point depth (Nuri et al., 2005)

The DBMS values may also be controlled by major lineaments and faulting, sub-crustal reworking, plume activities and the plate motion causing Himalayan orogeny (Bansal et al., 2013).

Geophysical survey is more appreciated when two or more geophysical methods are employed, therefore this research also undertook a further qualitative analysis of radiometric data over the study area of concentrations of Uranium, Thorium and Potassium with high heat flow and geothermal gradients to correlate and complement the result obtained from the analysis of Aeromagnetic data.

In thermally normal continental regions, the average heat flow is about 60mWm^{-2} . Values between $80\text{-}100\text{ mWm}^{-2}$ are good geothermal source, while values greater than 100m Wm^{-2} indicate anomalous conditions (Cull and

conley, 1983; Jessop *et al.*, 1976).

Location of the study area

The study area covers the eastern part of lower Benue trough, it is bounded by latitude 7.00° and 8.00° and longitude 8.00° and 9.50° (figure 1.0) and six HR aeromagnetic map sheets number 250, 251, 252, 270, 271 and 272, with a total area of $18,150\text{ km}^2$, cover part of Markudi, Gboko, Otukpo Agena, Akwana, and Katsina-Ala. The physiological features recognized in the area is the river Benue running over the upper part of the study area. The major factor that influenced the choice of the location for the research was the sitting of Akiri warm spring 43°C around the Benue Trough and Ruwan Zafi spring 54°C at the Northern part of Benue Trough.

Brief geology of the study area

The geology map of the study area Figure 1 shows that the western part of the study area host Sedimentary formation of middle Eocene age (sandstone, clay and limestone) and the eastern part host the undifferentiated old biotite granites.

Benue trough is known to be major structural feature in the Eastern part of Nigeria and an important element in the tectonic framework of Africa and the entire Benue Trough is believed to have evolved as a result of the continental separation of Africa and South America (King, 1950), and is variously described as a rift system (Cratchley and Jone, 1965), an extensional graben system (Stoneley, 1966; Wright, 1968), a third failed arm or anaulacogen of a three-armed rift system related to the development of domes associated with hotspots (Burke, 1976; Olade, 1978).

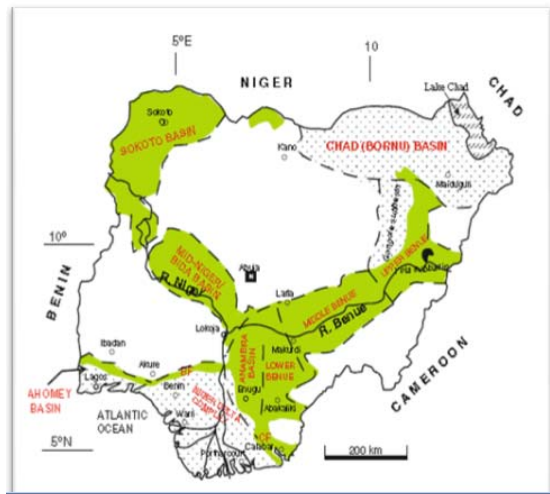


Figure 1: Geology map of Nigeria showing the location of Benue Trough (NGSA)

Sedimentation in the Lower Benue Trough commenced with the marine Albian Asu River Group, although some pyroclastics of Aptian – Early Albian ages have been sparingly reported (Ojoh, 1992). The marine Cenomanian – Turonian Nkalagu Formation (black shales, limestones and siltstones) and the interfingering regressive sandstones of the Agala and Agbani Formations rest on the Asu River Group. Mid-Santonian deformation in the Benue Trough displaced the major depositional axis westward which led to the formation of the Anambra Basin. Post-deformational sedimentation in the Lower Benue Trough, therefore, constitutes the Anambra Basin. Rock type at the Eastern portion of the study area is identified as undifferentiated Older granite, mainly porphyritic granitized gneiss with porphyroblastic granite (Figure 2). Rock type at the western portion is identified as Gwandu formation of middle Eocene age of (sandstone, clay and limestone) on the Asu group are the lithologic units at the surface within the sedimentary basin. River Alluvium deposition identified along the river channel.

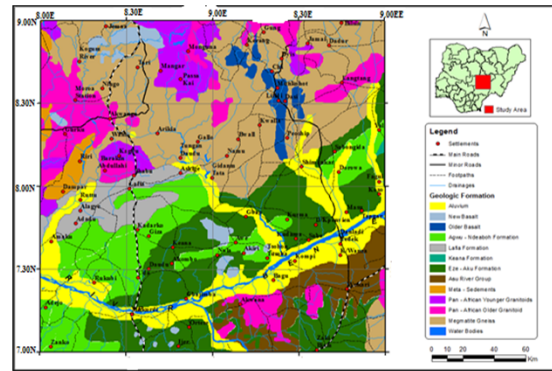


Figure 2: A simplified Geology map of the Study Area

2. METHODS

The calculation of DBMS in this study is based on statistical methods of depth determination from the radial power spectrum of the magnetic field (Spector and Grant, 1970; Bhattacharyya and Leu, 1975; Okubo et al., 1985, Blakely, 1995; Tanaka and Matsubayashi, 1999; Ross *et al.*, 2006; Trifonova *et al.*, 2009; Bensal *et al.*, 2011; Bensal *et al.*, 2013). These approaches assumed a random uniform uncorrelated distribution of sources. The power spectrum, P , for a 2D assemblage of bodies can be written as follow (Spector and Grant, 1970; Blakely, 1995).

$$P(k_x, k_y) = 4\pi^2 C_m^2 |\theta_m|^2 |\theta_f|^2 e^{-(1 - e^{-|k|} (z_t - z_b))} \quad (1)$$

Here, k_x and k_y are the wave numbers in the x - and y -directions; C_m is a constant of proportionality; θ_m is the power spectrum of the magnetization; θ_m and θ_f are the directional factors related to the magnetisation and geomagnetic field respectively; and z_t and z_b are the top and bottom depths of the magnetic sources. After annual averaging, Eq. (1) can be written as:

$$P|k| = A_1 e^{-2|k|Z_0} (1 - e^{-|k|(Z_0 - Z_c)})^2 \quad (2)$$

Where A_1 is a constant, k is the wave number and $P|k|$ power spectral density Equation (2) can be simplified to compute the centroid depth Z_0 of the magnetic source from the low-wave number part of the power spectrum as follows:

The centroid depth is calculated from the low wave number part of the scaled power spectrum as

$$\ln(P(K)^{\frac{1}{2}}/K) = [K]Z_0 \quad (3)$$

Where \ln is the natural logarithm, $P(k)$ is the radially average power spectrum, k is the wavenumber ($2\pi/\text{km}$). A is a constant depending on the properties of magnetization and its orientation and Z_0 is the centroid depth of the magnetic sources (Tanaka and Matsubayashi, 1999). For the high wave number part, the lower spectrum can be related to the top of magnetic sources by a similar equation:

$$\ln(P(K)^{\frac{1}{2}}/K) = [K]Z_1 \quad (4)$$

Where B is a constant: Z_1 is the depth to the top of the magnetic sources. The depth of the bottom of magnetisation Z_b is:

$$Z_b = 2Z_0 - Z_c \quad (5)$$

Summarily, the depth to the base of the magnetic source (i.e. the Curie point depth) is calculated in four steps (Tanaka and Matsubayashi, 1999) as follows:

Step 1: Calculate the radially averaged power spectrum of the magnetic data in each window;

Step 2: Estimate the depth to the top of the magnetic source (Z_c) using the high wave number portion of the magnetic anomaly power spectra;

Step 3: Estimate the depth to the centroid of the magnetic source (Z_0) using a lower wave number portion of the magnetic anomaly power spectra; and,

Step 4: Calculate the depth to the base of the magnetic source (Z_b) using $Z_b = 2Z_0 - Z_c$. The value of Z_b is the Curie point depth/DBMS.

Also the heat flow of the study area which has an assumption that the direction of the temperature variation is vertical and the temperature gradient dT/dz is constant; Fourier's law takes the form:

$$q = -k dT/dz \quad (6)$$

where, q is heat flow and k is thermal conductivity.

The Curie temperature $\theta^{\circ}\text{C}$ can also be defined as:

$$\theta^{\circ}\text{C} = (dT/dz)d \quad (7)$$

Where, d is the curie-point depth (as obtained from the spectral magnetic analysis). Therefore the Geothermal gradient in the relation to the heat flow q . Tanaka *et al* 1999):

$$q = k \theta^{\circ}\text{C}/d \quad (8)$$

Geothermal gradient ($\frac{\theta^{\circ}\text{C}}{d}$) of the study area was further estimated using curie point temperature of 580°C and thermal conductivity of $2.5\text{Wm}^{-1}\text{C}^{-1}$ which is the average thermal conductivity for igneous rocks is used in the study as standard (Nwankwo *et al.*, 2009).

However, using an average thermal conductivity, value of $2.5\text{Wm}^{-1}\text{C}^{-1}$ (Nwankwo *et al.*, 2011; Tanaka *et al.*, 1999), we then calculate the value for $\frac{\theta^{\circ}\text{C}}{d}$ geothermal gradient in the study area using the empirical relation between, curie depth Temperature and depth as shown in (equation 9).

$$\frac{H}{P} = 580^{\circ}\text{C}/d \quad (9)$$

Radiometric data processing

The Terrestrial radiation is mostly produced by the decay of the three natural radio isotopes ^{232}Th , ^{238}U and ^{40}K .

As radioactive decay is a random process, smoothing was carried out on the data to remove the noise, and the accuracy of all measurements and estimation was governed by statistical laws. The profiles of counting rates are noisy and the data cannot be contoured until they have been smoothed.

Correction for variation in attitude, atmospheric radon and cosmic radiation are made on the data, the data is then processed to produce results which are expressed as concentration of ^{232}Th , ^{238}U and ^{40}K . This is based on calibration data collected over source of known ground concentration and radiation levels (Coetzee, 2008).

The Radiometric heat analysis according to Salem and Fairhead indicates that, radiometric heat production (H) is related to the decay of primarily, the radioactive isotopes ^{232}Th , ^{238}U and ^{40}K and can be estimated based on the concentration (C) of the respective elements through the expression:

$$H(\mu\text{W}/\text{m}^3) = P(9.52C_u + 2.56 C_{\text{Th}} + 3.48C_K) 10^{-5} \quad (10)$$

Where:

H = radioactive heat production

P = density of rock adapted from (Telford *et al.*, 1990), C_u , C_{Th} , C_K are concentrations of uranium, thorium and potassium respectively.

The concentration of the three radiometric elements is read from the radiometric map covering the study area with high geothermal gradient.

3. ANALYSIS AND INTERPRETATION

The Total Magnetic Intensity (TMI) map of the study area as shown in figure 3 indicate regions of high (H) and low (L) with a magnetic intensity values ranging from -691.5nT to 614.6 nT respectively. The high magnetic anomalies trends from the north-eastern to the south-western part of study area, also the low magnetic anomalies were found south, north-eastern part and edge of south-western part of the study area.

The high magnetic anomalies might be as a result of basement intrusion into the sedimentary while low magnetic anomalies are associated with the thick sedimentation.

The High resolution aeromagnetic (HRAM) data was interpreted quantitatively by subjecting it to fourier and Spectral depth analysis with the aim of determining the depth to basement as well as the basement morphology. The TMI was windowed into twelve overlapping windows or sub-sheets. Upon each of the windows Fast Fourier Transform (FFT) and subsequently spectral depth analysis was undertaken this art decomposed the anomalies into its energy and wave number components. Thereafter a plot involving Energy versus wave number in cycle/km was made. A straight line is then manually fit to the energy spectrum both in the higher and lower portion (Figure 4).

Basically, two depth source models; H_1 and H_2 were revealed and further estimation of heat flow, geothermal gradient and curie depth were carryout using equations 5, 8 and 9. The depth to the deeper magnetic bodies (H_1) figure 5, varies between 5.52 km and 9.63 km but with an average value of about 7.42km while the depth due to the shallow causative magnetic sources (H_2) figure 6 varies between 0.28 km and 0.36 km but with an average depth value of 0.31 km (Table 1).

The Curie point depth of the study area figure 7 shows that the depth varies from 9 km to 18.6 km from south to the south-eastern part. The most pronounced high Curie depths were found at lower edge of Gboko with an approximate depth 18.6 km.

Also, two Shallow curie-point depths were observed at the South-eastern part (Katsina-Ala) and South-western part (Oturkpo) of the study area with a depth of 9.0 km and 10.2 km respectively, which may be due to the some intriguing techno-thermal effect related to a combination of subsidence, uplift, faulting, compression and volcanism Bansal *et al.*, 2013

The heat flow, figure 8 is observed to have value range from 75 mWm⁻² to 153.35 mWm⁻² with an average value of 103.98 Wm⁻². Anomalous heat flow (153.36, 135.61mWm⁻²) observed both south-eastern (Katsina-Ala) and lower edge south-western (Oturkpo) were within the igneous rock that outcrop in the area, located within shallow Curie depths.

The lowest Heat flow value were observed at the lower edge of Gboko and Makurdi value at 75 mWm⁻² The geothermal gradient result Figure 9 has a range of 30°C/km to 61°C/km with an average value of 41.59 °C/km. High values of geothermal gradients were recorded at the extreme edge of south-eastern part and lower edge of south-western part of the study. Figure 3, TMI map with the area location within the study area with IGRF of 33000 nT removed from the field values

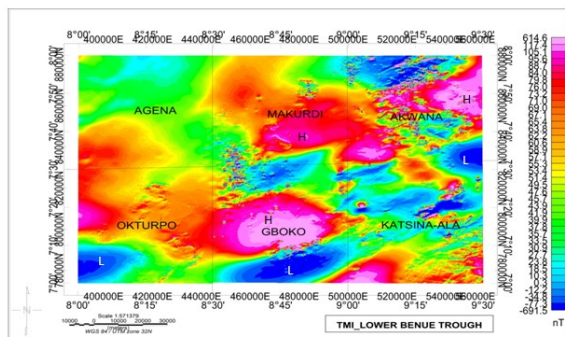


Figure 3: TMI map with area Location

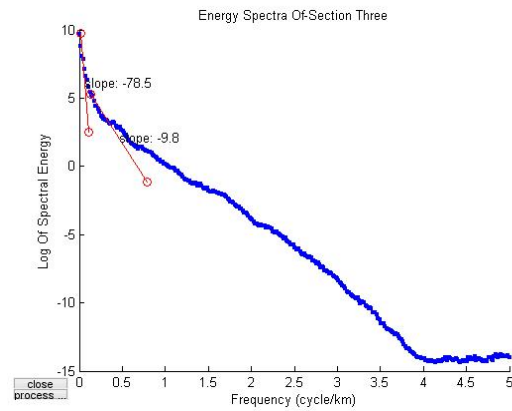


Figure 4: The plot of the log of spectral energy against frequency

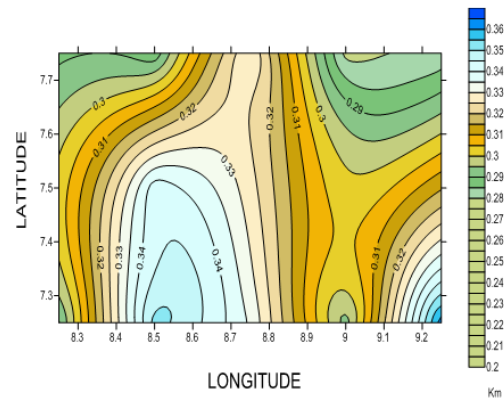


Figure 5: Shallow depths contour map of the study area

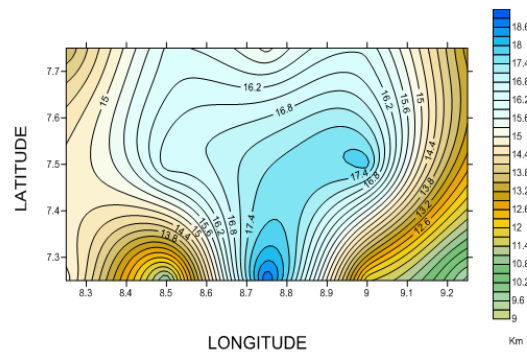


Figure 6: The Currie Point Depth contour map of the study area

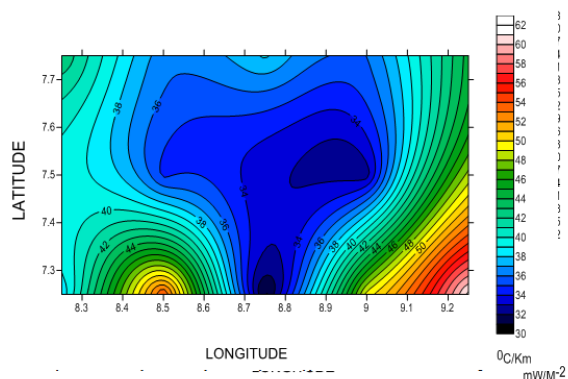


Figure 7: The Heat Flow contour map of the study area

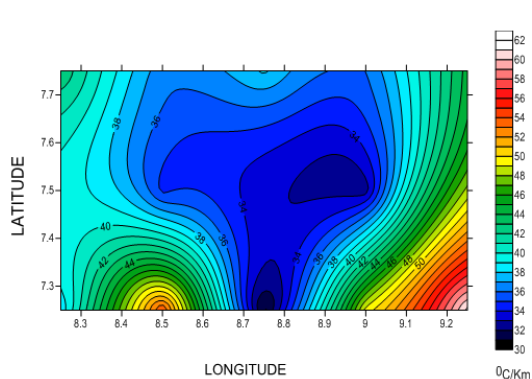


Figure 8: The geothermal gradient contour map of the study area

| SECT N | LAT (°N) | LONG (°E) | GRADIENT (D1) | DEPTH H1 (Km) | GRADIENT (D2) | DEPTH H2 (Km) | CURIE-POINT (Km) | GEOETHER GRADI (°C/km) | HEAT FLOW (mW/m ²) |
|--------|----------|-----------|---------------|---------------|---------------|---------------|------------------|------------------------|--------------------------------|
| 1 | 7.25 | 8.25 | 97.00 | 7.718 | 3.64 | 0.290 | 15.146 | 38.293 | 95.732 |
| 2 | 7.25 | 8.75 | 121.00 | 9.628 | 4.20 | 0.334 | 18.921 | 30.654 | 76.634 |
| 3 | 7.25 | 9.25 | 61.70 | 4.909 | 4.56 | 0.363 | 9.456 | 61.338 | 153.346 |
| 4 | 7.75 | 8.25 | 86.80 | 6.906 | 3.63 | 0.289 | 13.524 | 42.887 | 107.217 |
| 5 | 7.75 | 8.75 | 97.50 | 7.758 | 4.15 | 0.330 | 15.185 | 38.195 | 95.487 |
| 6 | 7.75 | 9.25 | 83.80 | 6.668 | 3.54 | 0.283 | 13.054 | 44.432 | 111.079 |
| 7 | 7.25 | 8.50 | 69.40 | 5.522 | 4.42 | 0.352 | 10.692 | 54.245 | 135.612 |
| 8 | 7.25 | 9.00 | 75.60 | 6.015 | 3.68 | 0.293 | 11.738 | 49.413 | 123.533 |
| 9 | 7.75 | 8.50 | 102.00 | 8.116 | 3.60 | 0.286 | 15.945 | 36.375 | 90.936 |
| 10 | 7.75 | 9.00 | 103.00 | 8.195 | 3.50 | 0.278 | 16.112 | 35.997 | 89.993 |
| 11 | 7.50 | 8.50 | 107.00 | 8.514 | 4.31 | 0.343 | 16.684 | 34.763 | 86.907 |
| 12 | 7.50 | 9.00 | 114.00 | 10.567 | 18.50 | 2.944 | 18.189 | 31.887 | 79.718 |

The correlation of Ternary count map and geothermal gradient.

The ternary map of the study area Figure 10 which is obtained by combining the potassium, thorium and uranium concentration of the area, concentration of each element is shown in distinct colour aggregate with potassium as red thorium as blue and uranium as green, value of concentration of each element (in Emu) are shown on the legend. The potassium concentration is high at the south-eastern part (Katsina-Ala) of the area which hosts undifferentiated old biotite-granites and a pronounced Thorium concentration at the western edge of Oturkpo which host the Emu formation (sandstone, clay and limestone) of Asu group, the ternary map shows relatively high concentration of potassium and Thorium, which indicate that the source of high geothermal values in this region could be traced to the contents of the geological structures.

From the concentration of each of these radioactive elements in the two geothermal active areas, Katsina-Ala and Oturkpo, the estimated radioactive heat production calculated using equation 10 are 1.47 $\mu\text{W}/\text{m}^3$ and 2.21 $\mu\text{W}/\text{m}^3$ respectively.

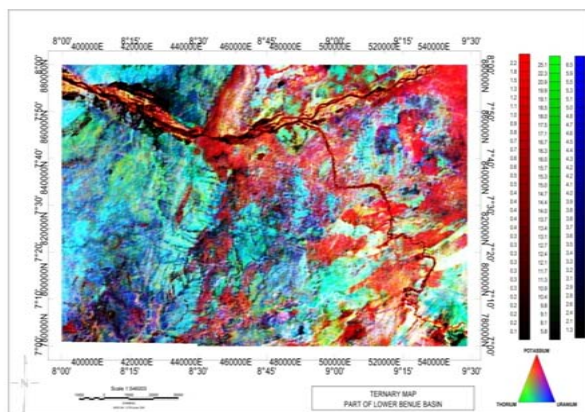


Figure 9: The Ternary count map of the study area

4. Conclusion

The spectral analysis of the aeromagnetic data shows that depth to the deeper magnetic bodies (H_1) varies between 5.52 km and 9.63 km with an average depth value of about 7.42 km, while the depth due to the shallow causative magnetic sources (H_2) Figure 6 varies between 0.28 km and 0.36 km with an average depth value of 0.31 km. The Curie-point depth varies from 9 km to a shallow depth of 19.5 km, shallowest curie depths values were recorded at the south-western part, around Oturkpo and south-eastern part of Katsina-Ala of the study area.

The Heat Flow value ranges from 75 mWm^{-2} to 153.35 mWm^{-2} with an average value of 103.98 Wm^{-2} . Anomalous Heat flows with values from 135.61 to 153.36 mWm^{-2} were observed at the south-eastern part around Katsina-Ala and the south-western part within Oturkpo, where igneous rocks outcrop in the area. The lowest Heat flow value was observed at the lower edge of Gboko and Makurdi with value around 75 mWm^{-2} . The geothermal gradient result has a range of 30°C/km to 61°C/km with an average value of 41.59°C/km. High values of geothermal gradients were recorded at the extreme edge of south-eastern part and the lower edge of south-western part of the study area with values of 62°C/km and 54°C/km respectively. The Lowest geothermal gradients were observed at lower edge of Gboko at 30°C/km and Makurdi at 34°C/km

The ternary count map of the study area which shows a distinct concentration of potassium content at the eastern part and thorium content at western part of the study area with a striking correlation between the region where the high geothermal gradient were observed and where the potassium concentration is high at the south-eastern part (Akwana and Katsina-Ala) of the area which host undifferentiated old biotite granites and a pronounced Thorium concentration at the western edge (Agena and

Oturkpo) of the study area which host Emu formation (sandstone, clay, gravel and limestone) of western Nigeria.

Therefore the south-eastern part (Katsina-Ala) and lower edge of the south-western part (Oturkpo) of the study area could be a viable site for geothermal exploration. The radioactive heat production in these two areas was estimated to be $1.47 \mu\text{W}/\text{m}^3$ and $2.21 \mu\text{W}/\text{m}^3$ respectively.

References

- Abraham, E.M. Lawal, K.M. Ekwe, A.C. Alile. O. Murana, K.A. Lawal, A.A. (2014). Spectral analysis of aeromagnetic data for geothermal energy investigation of Ikogosi Warm Spring, Ekiti State, southwestern Nigeria. *Geothermal Energy* 2, pp. 1-21.
- Adedapo, J.O. Kurowska, E. Schoeneich. K, and Ikpokonte, A. (2013). E.Geothermal gradient of the Niger Delta from recent studies, *International Journal of Scientific & Engineering Research*, Volume 4, Issue 11 (2013), pp. 1-5.
- Bansal, A.R., Anand, S.P., RajaramMita, Rao V.K., Dimri, V.P. (2013). Depth to the bottom of magnetic sources (DBMS) from aeromagnetic data of central India using modified centroid method for fractal distribution of sources. *Tectonophysics*, 603 (2013): 155-161.
- Bansal, A. R., Gabriel, G., Dimri, V. P. and Krawczyk, C. M. (2011). Estimation of depth to the bottom of magnetic sources by a modified centroid method for fractal distribution of sources: An application to aeromagnetic data in Germany, *Geophysics*, 76(3) L11–L22, 10.1190/1.3560017
- Bansal, A.R., Anand, S.P., Rajaram Mita, Rao V.K., Dimri, V.P. (2013). Depth to the bottom of magnetic sources (DBMS) from aeromagnetic data of central India using modified centroid method for fractal distribution of sources. *Tectonophysics*, 603 (2013): 155-161
- Bhattacharryya, B.K. and L.K. Leu (1975). Spectral analysis of gravity and Magnetic anomalies due two dimensional structures, *Geophysics*, Vol. 40pp. 993-1031.
- Blakely, R.J. (1995). Potential theory in gravity and magnetic applications. Cambridge University Press, Cambridge.
- Blakely, R.J. (1995). Potential theory in gravity and magnetic applications. Cambridge University Press, Cambridge.
- Burke, K. (1976). The Chad Basin: An active intra-continental basin. *Tectonophysics*, 36, 197-206.
- Coetzee, H. (2008). Acquisition, processing and enhancement of multi-channel radiometric data collected with ultralight aircraft mounted detectors. School of Geosciences University of the Witwatersrand, Johannesburg. PhD: 357pp. Google Scholar.
- Cratchley, C. R and Jones, G. P. (1965). An interpretation of the Geology and Gravity Anomalies of the Benue Valley Nigeria British Oversea. Geol. Survey Geophysics Paper No. 1, 126.
- Cull, J. P. and D. Conley (1983). Geothermal Gradients and Heat Flow in Australian Sedimentary Basin. *Journal of Australian Geology & Geophysics*, 8 (1983): 32-337.
- Henrik, ErlingNaess and Jan E. Evensen. (2012). Thermal modeling in the Oslo Rift, Norway. Thirty-seventh workshop on Geothermal Reservoir Engineering Stanford University, p. 194.
- Jessop, A.M., M.A. Habart and J.G. Sclater, (1976). The world heat flow data collection 1975. Geothermal services of Canada. Geotherm Ser., 50: 55-77.
- King, L. C. (1950). Outline and Description of Gondwanaland. *Geological Magazine*,. Vol. 87, pp. 353-359.
- Megwara John, U., Emmanuel E. Udensi, Peter I. Olasehinde, Mohammed A. Daniyan &

- Kolawole M. Lawal (2013). Geothermal and radioactive heat studies of parts of southern Bida basin, Nigeria and the surrounding basement rocks, *International Journal of Basic and Applied Sciences*, 2(1), pp. 125-139.
- Nagata, T. (1961). Rock Magnetism, Maruzen, Tokyo. Nnange, J.M, poudjom Djomani, p. 350.
- Nuri, D.M, Timur, U.Z, Mumtaz, H, Naci, O. (2005). Curie Point Depth variations to infer thermal structure of the crust at the African- Eurasian convergence zone, SW.
- Nwankwo, L.I, Olasehinde, P.I and Akoshile, C.O. (2011), Heat flow anomalies from the spectral analysis of Airborne Magnetic data of Nupe Basin, Nigeria. *Asian Journal of Earth Sciences*. Vol.1. No.1pp. 1-6
- Nwankwo, L.I., P.I. Olasehinde and C.O. Akoshile. (2009): An attempt to estimate the Curie-point isotherm depths in the Nupe Basin, West Central Nigeria. *Global J. Pure Applied Sci.*, 15427-433.
- Ofor, Ngozi, P. and Udensi, Emmanuel, E. (2014). Determination of the Heat Flow in the Sokoto Basin, Nigeria using Spectral Analysis of Aeromagnetic Data, *Journal of Natural Sciences Research*, Vol.4, No.6 pp. 83-86.
- Ojoh, K.A. (1992). The Southern part of the Benue Trough (Nigeria) Cretaceous stratigraphy, basin analysis, paleo-oceanography and geodynamic evolution in the equatorial domain of the South Atlantic, Vol. 7, pp. 131-152.
- Okubo, Y., R. J. Graf, R. O. Hansen, K. Ogawa, and H. Tsu (1985). Curie point depths of the island of Kyushu and surrounding area, Japan: *Geophysics*, 50, no. 3481-489, doi:10.1190/1.1441926
- Olade, M. A. (1991). Early cretaceous basaltic volcanism and initial continental rifting in benue trough. *Journal of mining geology* 16 (1978), 17-25.
- Ross, H. E., R. J. Blakely, and M. D. Zoback, (2006) Testing the use of aeromagnetic data for the determination of Curie depth in California: *Geophysics*, 71, no. 5, L51–L59, doi:10.1190/1.2335572
- Salem, A. & Fairhead, D. (2011). Geothermal reconnaissance of Gebel Duwi area, Northern Red Sea, Egypt using airborne magnetic and spectral gamma ray data. *Getech.*, pp.1-22.
- Spector, A. and Grant, F.S. (1970). Statistical models for interpreting aeromagnetic data, *Geophysics*, Vol.35, pp. 293-302.
- Stoneley, R. (1966). The Niger Delta region in the light of the theory of continental drift *Geol. Mag.*, 103, pp 385-397.
- Tanaka, A. Y. Okubo and O. Matsubayashi. (1999) Curie point depth based on spectrum analysis of the magnetic anomaly data in East and Southeast Asia, *Tectonophysics*, Vol.306, pp 461-470.
- Telford, W. M., Geldart, L. P., Sherif, R. E. and Keys, D. A. (1990). *Applied Geophysics*. Cambridge: Cambridge University Press.
- Trifonova, P., Z. Zhelev, T. Petrova, and K. Bojadgieva (2009). Curie point depths of Bulgarian territory inferred from geomagnetic observations and its correlation with regional thermal structure and seismicity: *Tectonophysics*, 473, No. 3-4, pp, 362-374, doi:10.1016/j.tecto.2009.03.014
- Tselentis, G. A. (1991). An attempt to define curie depths in Greece from aeromagnetic and heat flow data. *PAGEOPH* 136:87-101.
- Wright, J.E. (1968). The geology of church stretton area. Institute of geological sciences (geological survey of Great Britain), vi (1968) +87p., with 4 figs. HMSO, London.
- Wright, J.E. (1968). The geology of church stretton area. Institute of geological sciences (Geological Survey of Great Britain), vi +87p., HMSO, London.